Available online at www.sciencedirect.com
SCIENCE DIRECT®
Applied Acoustics 67 (2006) 185–200
applied acoustics
www.elsevier.com/locate/apacoust

Energy transmission through a double-wall structure with an acoustic enclosure: Rotational effect of mechanical links

Y.Y. Li, L. Cheng *

Department of Mechanical Engineering, The Hong Kong Polytechnic University, Hung Hom, Kowloon, Hong Kong SAR, China

Received 26 May 2005; received in revised form 13 June 2005; accepted 13 June 2005
Available online 22 August 2005

Abstract

This paper investigates the rotational effect of mechanical links on energy transmission of a double-wall structure with an enclosure. A criterion is proposed to identify energy transmission mechanisms and predict the dominant transmitting path. Studies in different frequency ranges show a more significant energy transmission due to the rotational effect of the link at higher frequencies compared with lower ones. Comparison between the translational effect and the rotational effect on energy transmission shows that although both effects are important for the transmission mechanism analysis, the rotational effect on energy transmission is more remarkable at high frequencies for a soft translational link; whereas is insensitive for a stiff one.

Keywords: Energy transmission; Rotational effect; Double-wall structure; Links

1. Introduction

Energy transmission through double-wall structures has been widely studied during the past decades [1,2]. A clear understanding of the energy transmission

* Corresponding author. Tel.: +852 2766 6769; fax: +852 2365 4703.
E-mail address: mmlcheng@polyu.edu.hk (L. Cheng).

0003-682X/$ - see front matter © 2005 Elsevier Ltd. All rights reserved.
doi:10.1016/j.apacoust.2005.06.004

mechanism between the two panels is essential for vibroacoustic analysis or active noise control of such structures [3–10]. Most previous work focused on structures without any mechanical joints between the two walls, in which energy is entirely transmitted through the air gap, forming the acoustic transmitting path. Recently, studies on energy transmission between the two panels connected with mechanical links or connectors have been presented [11–16]. For example, Lin et al. [11] investigated the transmission of a plane sound wave through two infinite parallel plates connected by identical periodically spaced frames, and also compared the strengths of the two transmission paths (structural path through the studs and the airborne path through the cavity). Bao et al. [12] experimentally examined the effect of the mechanical path on sound transmission through double walls for active acoustic control applications. It was observed that, in some circumstances, a significant portion of energy could be transmitted from these links, referred to as structural transmitting path. In general, a realistic mechanical link conveys energy between the two panels through transverse forces and the moments, which are caused by the translational and rotational effects of the link, respectively. Effects of the translational link on energy transmission have been extensively investigated in [13–16]. In our previous work [13], the respective effects of the air gap and the links on energy transmission and noise insulation properties have been assessed. It was observed that the translational stiffness of the mechanical link and the aerostatic stiffness of the air gap are the two parameters governing the energy transmission process. A criterion was also proposed to analyze different transmission mechanisms and then to predict the dominant transmitting path.

As far as the rotational effect on sound/vibration transmission is concerned, there is a considerable amount of literature dealing with other configurations such as beams or plate-like structures [17–21]. For example, Petersson et al. and Sanderson et al. [17–19] investigated the important role played by the moment excitation in vibration transmission in built-up structure. Koh et al. [20] claimed that both force and moment excitations are critical in the energy transmission through beams or plate-like structures, in which moment excitations were considered through moment mobilities using Rayleigh–Ritz method. Gardonio et al. [21] studied translational and rotational excitations in the energy transmission of a vibrating mass isolated from a finite plate, and showed that at high frequencies, the energy was transmitted through axial and angular vibration simultaneously. Investigations by Goyder and White [22] revealed that, in the high frequency region, the vibrational power input to a beam or a plate due to a moment excitation exceeds that due to a force excitation. All these evidences suggest that the rotational effect is important to be considered in sound/vibration transmission analysis.

Compared with aforementioned configurations, double-plate structures with rotational links, however, received much less attention. One of a very few existing examples is the work of Takahashi [23], in which the sound radiation from periodically connected infinite double-panel structures were investigated. That work concluded that the stiffness of the connectors has important effects upon the radiated power. However, no systematic analysis has been reported so far to investigate the rotational effect of links on energy transmission for a double-wall structure coupled with

an acoustic enclosure. Criteria to identify the dominating transmitting mechanism are also lacking. In addition, the relative importance of the translational effect and the rotational effect on energy transmission also needs to be clarified in different frequency regions.

This paper attempts to answer these questions using a mechanically linked double-wall structure, radiating sound into a rectangular enclosure. A brief description of the modeling process is first presented. Numerical studies are then conducted to investigate the rotational effect on energy transmission and noise insulation properties. Based on an index defined as the ratio between the rotational stiffness of the link and the aerostatic stiffness of the air gap, a criterion for predicting the dominant transmission path is proposed. The relationship between the rotational effect and the translational effect on energy transmission is explored in different frequency regions. Finally, some conclusions are drawn.

2. Formulation

Consider a mechanically linked double-wall structure connected to an acoustic enclosure as shown in Fig. 1. The double-wall structure is composed of two homogeneous and isotropic rectangular panels a (upper) and b (lower), which are simply supported along their boundaries and separated by an air gap cavity with a volume V_g and a thickness h_g. A mechanical link is located at (x_m, y_m) to connect these two panels. Apart from the surfaces occupied by the two panels, all other surrounding walls of the air gap and the enclosure are acoustically rigid.

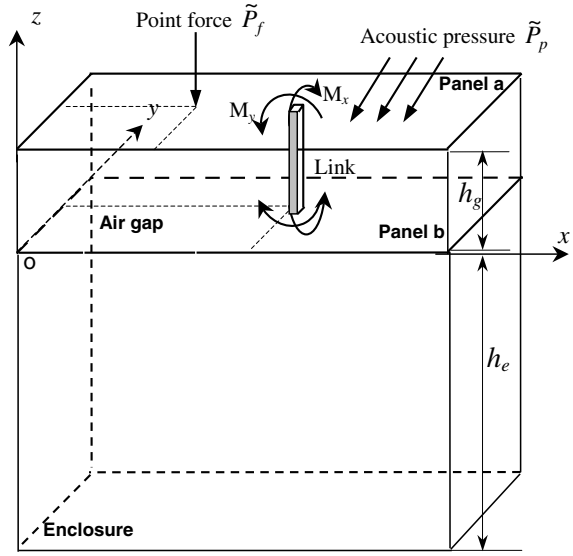

Fig. 1. A mechanically linked double-wall structure.

As the first step of energy transmission analysis, a vibroacoustic model, which includes the vibration of the two panels and the acoustic pressure inside the air gap and the enclosure, is established. For panel a, the equation of motion under an external excitation, which can either be a point force $\widetilde{P}_{\mathrm{f}}$ at $(x_{\mathrm{f}}, y_{\mathrm{f}})$ or an acoustic pressure $\widetilde{P}_{\mathrm{p}}$, is expressed as

$$\begin{aligned} D_{\mathrm{a}}\nabla^4 w_{\mathrm{a}} + \rho_{\mathrm{a}} h_{\mathrm{a}} \frac{\partial^2 w_{\mathrm{a}}}{\partial t^2} = {} & \widetilde{P}_{\mathrm{f}}\delta(x - x_{\mathrm{f}}, y - y_{\mathrm{f}}) + \widetilde{P}_{\mathrm{p}} - f_{\mathrm{m}} \cdot \delta(x - x_{\mathrm{m}}, y - y_{\mathrm{m}}) \\ & - M_x \cdot \delta(x - x_{\mathrm{m}})\delta'(y - y_{\mathrm{m}}) - M_y \cdot \delta'(x - x_{\mathrm{m}})\delta(y - y_{\mathrm{m}}) \\ & - P_{\mathrm{g}}(z = h_{\mathrm{g}}), \end{aligned} \tag{1}$$

and for panel b,

$$\begin{aligned} D_{\mathrm{b}}\nabla^4 w_{\mathrm{b}} + \rho_{\mathrm{b}} h_{\mathrm{b}} \frac{\partial^2 w_{\mathrm{b}}}{\partial t^2} = {} & f_{\mathrm{m}} \cdot \delta(x - x_{\mathrm{m}}, y - y_{\mathrm{m}}) + M_x \cdot \delta(x - x_{\mathrm{m}})\delta'(y - y_{\mathrm{m}}) \\ & + M_y \cdot \delta'(x - x_{\mathrm{m}})\delta(y - y_{\mathrm{m}}) + P_{\mathrm{g}}(z = 0) - P_{\mathrm{e}}(z = 0), \end{aligned} \tag{2}$$

where $(w_{\mathrm{a}}, D_{\mathrm{a}}, \rho_{\mathrm{a}}, h_{\mathrm{a}})$ and $(w_{\mathrm{b}}, D_{\mathrm{b}}, \rho_{\mathrm{b}}, h_{\mathrm{b}})$ are the transverse displacements (positive downwards), the flexible rigidities, the densities and the thicknesses of panels a and b, respectively. δ is the Dirac delta function representing the concentrated source while δ' is its derivation describing the moment. P_{g} and P_{e} are the acoustic pressures inside the air gap and the enclosure, respectively. f_{m}, M_x and M_y are the force, the rotational moments about the x- and y-axis caused by the mechanical link, respectively. They can be simulated by a spring having a translational stiffness K_{m} as

$$f_{\mathrm{m}} = K_{\mathrm{m}}[w_{\mathrm{a}}(x_{\mathrm{m}}, y_{\mathrm{m}}) - w_{\mathrm{b}}(x_{\mathrm{m}}, y_{\mathrm{m}})], \tag{3a}$$

and an equal rotational stiffness C_{m} in x- and y-directions as

$$M_x = C_{\mathrm{m}}\theta_x, \quad M_y = C_{\mathrm{m}}\theta_y. \tag{3b}$$

In Eq. (3b), θ_x and θ_y are the angular rotations described as

$$\begin{aligned} \theta_x &= \frac{\partial w_{\mathrm{a}}(x_{\mathrm{m}}, y_{\mathrm{m}}, t)}{\partial y} - \frac{\partial w_{\mathrm{b}}(x_{\mathrm{m}}, y_{\mathrm{m}}, t)}{\partial y}, \\ \theta_y &= -\left(\frac{\partial w_{\mathrm{a}}(x_{\mathrm{m}}, y_{\mathrm{m}}, t)}{\partial x} - \frac{\partial w_{\mathrm{b}}(x_{\mathrm{m}}, y_{\mathrm{m}}, t)}{\partial x}\right). \end{aligned} \tag{4}$$

It is relevant to mention that the total pressure acting on the outer side of the panel a contains three parts, i.e. the incident pressure, the reflected pressure when the panel is assumed rigid and the radiated pressure due to vibration of the panel. The combination of the first two parts is usually referred to as the blocked pressure. It is generally accepted that, in air, the radiated pressure is rather low compared to the blocked pressure [10]. Therefore, the radiated pressure towards outside of the panel a is neglected in the present formulation.

Following the conventional modal superposition theory, w_{a} and w_{b} are decomposed over the mode shape functions $\varphi_{\mathrm{a},ij}(x, y)$ and $\varphi_{\mathrm{b},ij}(x, y)$ of panels a and b, respectively,

$$w_{\mathrm{a}}(x,y,t)=\sum_{i=1}^{\mathsf{M}}\sum_{j=1}^{\mathsf{N}}\varphi_{\mathrm{a},ij}(x,y)q_{\mathrm{a},ij}(t), \tag{5a}$$

$$w_{\mathrm{b}}(x,y,t)=\sum_{i=1}^{\mathsf{M}}\sum_{j=1}^{\mathsf{N}}\varphi_{\mathrm{b},ij}(x,y)q_{\mathrm{b},ij}(t), \tag{5b}$$

where $q_{\mathrm{a},ij}(t)$ (or $q_{\mathrm{b},ij}(t)$) is the ij-modal coordinate of panel a (or b). Using the orthogonality property of shape functions and considering the effect of viscous damping, Eqs. (1) and (2) can be expressed as

$$\begin{aligned}&\ddot{q}_{\mathrm{a},kl}(t)+2\zeta_{\mathrm{a},kl}\omega_{\mathrm{a},kl}\dot{q}_{\mathrm{a},kl}(t)+\omega_{\mathrm{a},kl}^2q_{\mathrm{a},kl}(t)\\&\quad=\frac{1}{m_{\mathrm{a},kl}}\left\{\int\int(\widetilde{P}_{\mathrm{p}}-P_{\mathrm{g}})\varphi_{\mathrm{a},kl}\,\mathrm{d}x\,\mathrm{d}y+\widetilde{P}_{\mathrm{f}}\varphi_{\mathrm{a},kl}(x_{\mathrm{f}},y_{\mathrm{f}})-f_{\mathrm{m}}\varphi_{\mathrm{a},kl}(x_{\mathrm{m}},y_{\mathrm{m}})\right.\\&\qquad-\int\int M_x\cdot\delta(x-x_{\mathrm{m}})\delta'(y-y_{\mathrm{m}})\varphi_{\mathrm{a},kl}\,\mathrm{d}x\,\mathrm{d}y\\&\qquad\left.-\int\int M_y\cdot\delta'(x-x_{\mathrm{m}})\delta(y-y_{\mathrm{m}})\varphi_{\mathrm{a},kl}\,\mathrm{d}x\,\mathrm{d}y\right\},\end{aligned} \tag{6}$$

$$\begin{aligned}&\ddot{q}_{\mathrm{b},kl}(t)+2\zeta_{\mathrm{b},kl}\omega_{\mathrm{b},kl}\dot{q}_{\mathrm{b},kl}(t)+\omega_{\mathrm{b},kl}^2q_{\mathrm{b},kl}(t)\\&\quad=\frac{1}{m_{\mathrm{b},kl}}\left\{\int\int(P_{\mathrm{g}}-P_{\mathrm{e}})\varphi_{\mathrm{b},kl}\,\mathrm{d}x\,\mathrm{d}y+f_{\mathrm{m}}\varphi_{\mathrm{b},kl}(x_{\mathrm{m}},y_{\mathrm{m}})\right.\\&\qquad+\int\int M_x\cdot\delta(x-x_{\mathrm{m}})\delta'(y-y_{\mathrm{m}})\varphi_{\mathrm{b},kl}\,\mathrm{d}x\,\mathrm{d}y\\&\qquad\left.+\int\int M_y\cdot\delta'(x-x_{\mathrm{m}})\delta(y-y_{\mathrm{m}})\varphi_{\mathrm{b},kl}\,\mathrm{d}x\,\mathrm{d}y\right\},\end{aligned} \tag{7}$$

where $\omega_{\mathrm{a},kl}$ (or $\omega_{\mathrm{b},kl}$) and $m_{\mathrm{a},kl}$ (or $m_{\mathrm{b},kl}$) are the klth natural angular frequency and the generalized mass of the klth mode of panel a (or b), respectively, $k=1,\ldots,\mathsf{M}$; $l=1,\ldots,\mathsf{N}$.

As far as the acoustic pressure P_{g} inside the gap cavity is concerned, one has the following classical wave equation and the associated constraint conditions based on velocity continuity:

$$\nabla^2P_{\mathrm{g}}-\frac{1}{c_{\mathrm{o}}^2}\frac{\partial^2P_{\mathrm{g}}}{\partial t^2}=0,\quad\frac{\partial P_{\mathrm{g}}}{\partial\mathbf{n}}=\begin{cases}\rho\ddot{w}_{\mathrm{a}} & \text{on panel a,}\\ -\rho\ddot{w}_{\mathrm{b}} & \text{on panel b,}\\ 0 & \text{on the rigid wall,}\end{cases} \tag{8}$$

where ρ and c_{o} are the equilibrium fluid density and the sound velocity within the cavity, respectively. $\mathbf{n}$ is the normal direction towards outside of the wall. Decomposing P_{g} on the basis of the acoustic mode shapes $\psi_{\mathrm{g},j}$ as $P_{\mathrm{g}}=\sum_j\psi_{\mathrm{g},j}p_{\mathrm{g},j}(t)$ and applying Green's theorem [24], Eq. (8) can be rewritten as

$$\ddot{p}_{g,j}(t) + 2\zeta_{g,j}\omega_{g,j}\dot{p}_{g,j}(t) + \omega_{g,j}^2 p_{g,j}(t) = \frac{\rho A c_o^2}{m_{g,jj} V_g}\left[\sum_{k=1}^{M}\sum_{l=1}^{N} L_{j,kl}^{ag}\ddot{q}_{a,kl}(t) - \sum_{k=1}^{M}\sum_{l=1}^{N} L_{j,kl}^{bg}\ddot{q}_{b,kl}(t)\right], \quad j = 1,\ldots,n_g, \tag{9}$$

by introducing a modal loss factor $\zeta_{g,j}$. In Eq. (9), $p_{g,j}(t)$, $\omega_{g,j}$ and $m_{g,jj}$ stand for the jth modal pressure amplitude, angular frequency and the generalized mass of the gap cavity, respectively. A is the area of the wall. $L_{j,kl}^{ag}$ and $L_{j,kl}^{bg}$ are the modal coupling coefficients. Similarly, the acoustic pressure P_e inside the enclosure satisfies

$$\ddot{p}_{e,j}(t) + 2\zeta_{e,j}\omega_{e,j}\dot{p}_{e,j}(t) + \omega_{e,j}^2 p_{e,j}(t) = \frac{\rho A c_o^2}{m_{e,jj} V_e}\sum_{k=1}^{M}\sum_{l=1}^{N} L_{j,kl}^{be}\ddot{q}_{b,kl}(t), \quad j = 1,\ldots,n_e. \tag{10}$$

In Eq. (10), symbols with subscript "e" have the same meaning as those defined above but apply to the enclosure. In the case of harmonic excitation, Eqs. (6), (7), (9) and (10) can be combined into matrix form after derivations (see Appendix), and the displacement of each panel and the acoustic pressures inside the air gap and the enclosure can therefore be calculated. It is pertinent to mention that the derived equations are cast in a general form, considering the rotational and translational effects simultaneously. Should only rotational effect be considered, Eqs. (6) and (7) can be further simplified by setting $K_m = 0$.

Vibrations of the two panels are examined using the averaged quadratic velocity defined as

$$\langle V_a^2\rangle = \frac{\omega^2}{2A}\int_A w_a w_a^* \,\mathrm{d}s, \quad \langle V_b^2\rangle = \frac{\omega^2}{2A}\int_A w_b w_b^* \,\mathrm{d}s \tag{11}$$

for panels a and b, respectively. The asterisk denotes complex conjugate. Based on the fact that the area under the spectrum of $\langle V^2\rangle$ roughly represents the energy level within the analyzed frequency range, energy transmission between the two panels can be characterized by

$$\gamma_{pl} = \frac{\rho_b h_b \overline{\langle V_b^2\rangle}}{\rho_a h_a \overline{\langle V_a^2\rangle}}, \tag{12}$$

where $\overline{\langle V_b^2\rangle}$ and $\overline{\langle V_a^2\rangle}$ are, respectively, the areas under the spectra $\langle V_b^2\rangle$ and $\langle V_a^2\rangle$ defined as

$$\overline{\langle V_b^2\rangle} = \int_{f_1}^{f_2}\langle V_b^2\rangle \,\mathrm{d}f, \quad \overline{\langle V_a^2\rangle} = \int_{f_1}^{f_2}\langle V_a^2\rangle \,\mathrm{d}f, \tag{13}$$

where $[f_1–f_2]$ is the frequency range of interest.

The acoustic insulation properties of the double-wall structure are then analyzed using the noise reduction index, γ_{NR}, defined as the difference between the sound pressure level at the top side of panel a and the averaged sound pressure level inside the enclosure as:

$$\gamma_{NR} = 10\log\left(\frac{\langle P_{out}^2\rangle}{P_{ref}^2}\right) - 10\log\left(\frac{\langle P_e^2\rangle}{P_{ref}^2}\right), \tag{14}$$

where $\langle P_{out}^2\rangle$ is the mean-square sound pressure averaged over the top side surface of panel a under an oblique incident plane wave excitation,

$$\langle P_{out}^2\rangle = \frac{1}{2A}\int_A P_{out}P_{out}^* \,\mathrm{d}s, \tag{15a}$$

$$\langle P_e^2\rangle = \frac{1}{2V_e}\int_{V_e} P_eP_e^* \,\mathrm{d}\upsilon, \quad p_{ref} = 20\ \mu\mathrm{Pa}. \tag{15b}$$

3. Results and discussions

Numerical simulations were performed to investigate the rotational effect on energy transmission between the two aluminum panels. Dimensions of the two panels are $0.5 \times 0.35 \times 0.002\ \mathrm{m}^3$ for the upper panel a, and $0.5 \times 0.35 \times 0.003\ \mathrm{m}^3$ for the lower one b (see Fig. 1). The depth of the enclosure is fixed at $h_e = 0.55$ m, while the depth of the air gap h_g is varied in different cases. A mechanical link, modeled as a spring with a translational stiffness K_m and a rotational stiffness C_m, is located at (0.3, 0.21) to connect the two panels. A harmonic excitation force with an amplitude of 1N is applied to panel a at (0.2, 0.14). Modal loss factors of 0.005 are assigned to both panels and 0.001 for the gap cavity and the enclosure. In the structural displacement and sound pressure decompositions, the number of modes used are (10,10) for the two panels, (9,7,2) for the gap cavity and (9,7,8) for the enclosure, which proved to be sufficient to properly cover the frequency range of interest.

3.1. Effect of the rotational moment on energy transmission

By neglecting the translational effect of the link ($K_m = 0$), the rotational effect on energy transmission is studied with $C_m = 10^3$ N/rad and $C_m = 0$. The averaged quadratic velocity of the two panels and the averaged sound pressure inside the cavities are plotted in Figs. 2(a) and (b), respectively. Comparing both cases shows a significant increase in the vibration energy transmission from panel a to b due to the rotational effect of the link (Fig. 2(a)). As a result, the averaged sound pressure inside the enclosure also increases. This increase is much more apparent at high frequencies, indicating an enhancing rotational effect on energy transmission as frequencies increase (Fig. 2(b)). Although the vibration level of panel a and the sound pressure level inside the air gap remain more or less the same before and after the consideration of C_m, resonance peaks are evidently altered, and some dominated by panel b can also be clearly identified in the spectra (denoted by a "•"), indicating a strong coupling between the two panels and a significant energy transmission due to the rotational effect of the link.

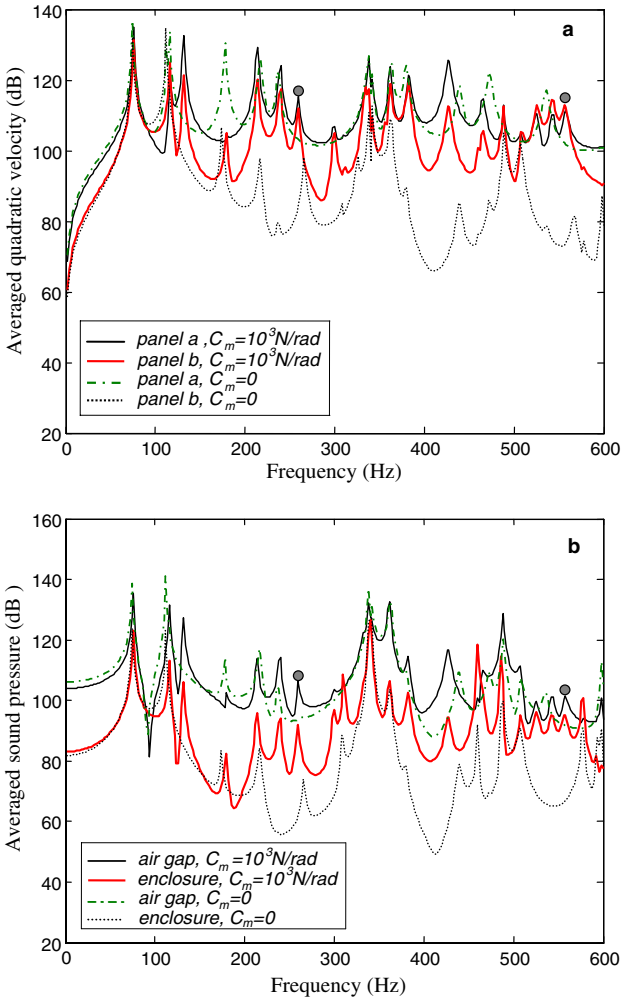

Fig. 2. Energy transmission without considering translational effect of the mechanical link when $h_g/h_e = 0.2$: (a). Averaged quadratic velocity of panels a and b; and (b). Averaged sound pressure level inside the air gap and the enclosure.

As reported in [13], the translational effect of mechanical links changes energy transmission mechanism, in which a criterion is presented to predict the dominant transmitting path. That criterion is revisited here by considering the rotational effect. Fig. 3(a) illustrates a tendency plot of γ_{pl} for different rotational stiffness with respect to h_g/h_e. Given a C_m, γ_{pl} first undergoes a subtle drop, then enters into a smooth drop region before finally reaching a plateau with the increase of h_g/h_e. The occurrence of each zone depends on the stiffness C_m. A stiffer link apparently pushes theses zones at lower h_g/h_e values. All curves exhibit the following characteristics: In the first zone, γ_{pl} is extremely sensitive to h_g/h_e, suggesting that a slight increase in h_g/h_e can result

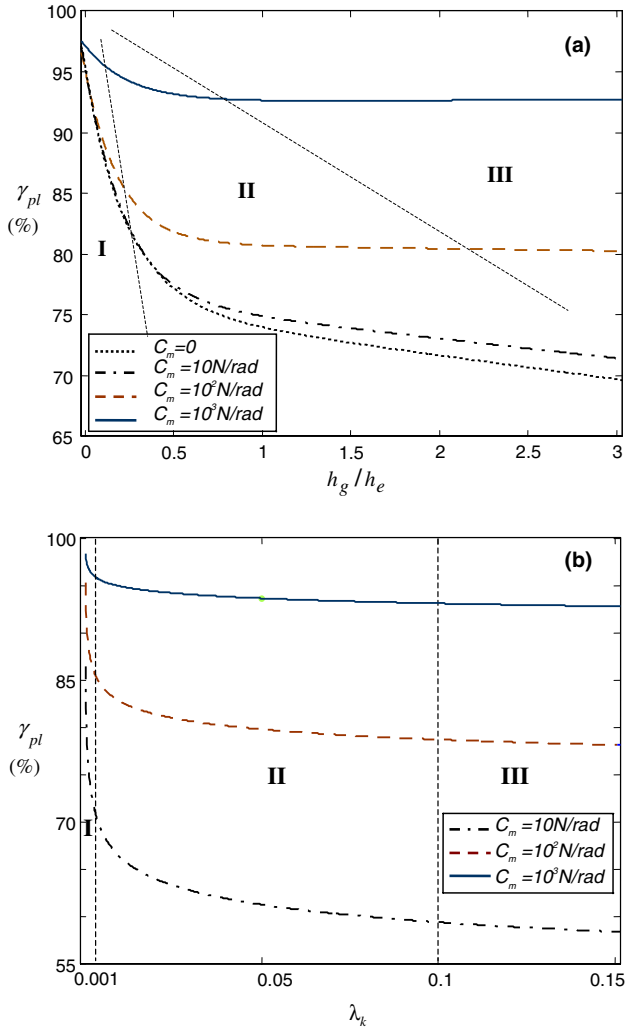

Fig. 3. Tendency plot of γ_{pl} showing the energy transmission between two walls: (a) with respect to h_g/h_e; and (b) with respect to λ_k.

in an obvious attenuation of the energy transmission between the two panels. This phenomenon is most remarkable with a soft link, with most of energy being transmitted through the air gap rather than the mechanical link. In the second zone, the gap effect is weakened and energy is transmitted through the link and the air gap simultaneously. In the third zone, γ_{pl} is insensitive to h_g/h_e, implying that the mechanical link dominates the energy transmission path.

Another observation is that, with an increasing C_m, γ_{pl} increases within a shortened first two zones and an elongated plateau zone, showing a remarkable rotational effect on energy transmission. Obviously, C_m and h_g are the two critical parameters

to separate these zones. Their effects on energy transmission can be better shown by defining a normalized parameter as

$$\lambda_k = \frac{C_m}{K_g}, \tag{16}$$

where K_g is the aerostatic stiffness of the gap cavity [13]

$$K_g \approx \rho c_o^2 A^2 (L_{o,11}^{bg})^2 / V_g, \tag{17}$$

in which $L_{o,11}^{bg}$ is the modal coupling coefficient between the cavity mode (0,0,0) of the air gap and the structural mode (1,1) of the panel b.

The tendency plot of γ_{pl} with respect to the normalized parameter λ_k is given in Fig. 3(b). Evidently, three zones can be systematically demarcated with rough delimitations at $\lambda_k = 0.001$ and 0.1. That is, when $\lambda_k \subset (0\,0.001]$, energy will be mainly transmitted from the acoustic path; while when $\lambda_k \subset [0.1\,\infty)$, the structural transmission is dominant; when $\lambda_k \subset [0.001\,0.1]$, energy is conveyed through both the acoustic and structural paths simultaneously. Although the demarcation lines are vague, this criterion can be used as a simple tool to roughly predict the main energy transmission path.

3.2. Noise reduction

Effects of transmission paths on noise reduction of the double-wall structure are investigated. An oblique plane wave having an amplitude of 1Pa, an elevation angle of 60° and an azimuth angle of 30° is exerted on panel a. Fig. 4(a) illustrates the noise reduction index γ_{NR} when $h_g/h_e = 0.2$ for three different cases: $C_m = 0$, 25 and 10^3 N/rad. Comparison between the curve for $C_m = 25$ N/rad with that for $C_m = 0$ shows that both curves almost coincide with each other. The reason is that the normalized parameter λ_k ($=6.8 \times 10^{-4}$) falls into zone I, in which energy is mostly transmitted through acoustic path. Such a soft link, therefore, has negligible effect on noise reduction. When C_m is increased to 10^3 N/rad (corresponding to $\lambda_k = 2.7 \times 10^{-2}$), however, except for the *first two* modes of the coupled system dominated by the two panels, a clear decrease in γ_{NR} is observed, meaning that most energy is transmitted through rotational moments, resulting in a much reduced noise insulation.

Fig. 4(b) shows the variation of γ_{NR} when $C_m = 10^2$ N/rad with: (1) $h_g/h_e = 0.05$ (in vacuo); (2) $h_g/h_e = 0.05$ ($\lambda_k = 6.8 \times 10^{-4}$) and (3) $h_g/h_e = 0.25$ ($\lambda_k = 3.4 \times 10^{-3}$). The obvious difference between the two cases with shallow gaps ($h_g/h_e = 0.05$) with and without air indicates a significant energy transmission through the acoustic path. When h_g/h_e is increased to 0.25, γ_{NR} curve approaches the in vacuo one. This is understandable because the increase in the gap depth weakens acoustic transmitting path, accompanied by a more dominant energy transmission through the link.

3.3. Rotational effect vs. frequencies

Rotational effect on energy transmission in different frequency regions is investigated. Two representative frequency bands are chosen for this purpose: a lower

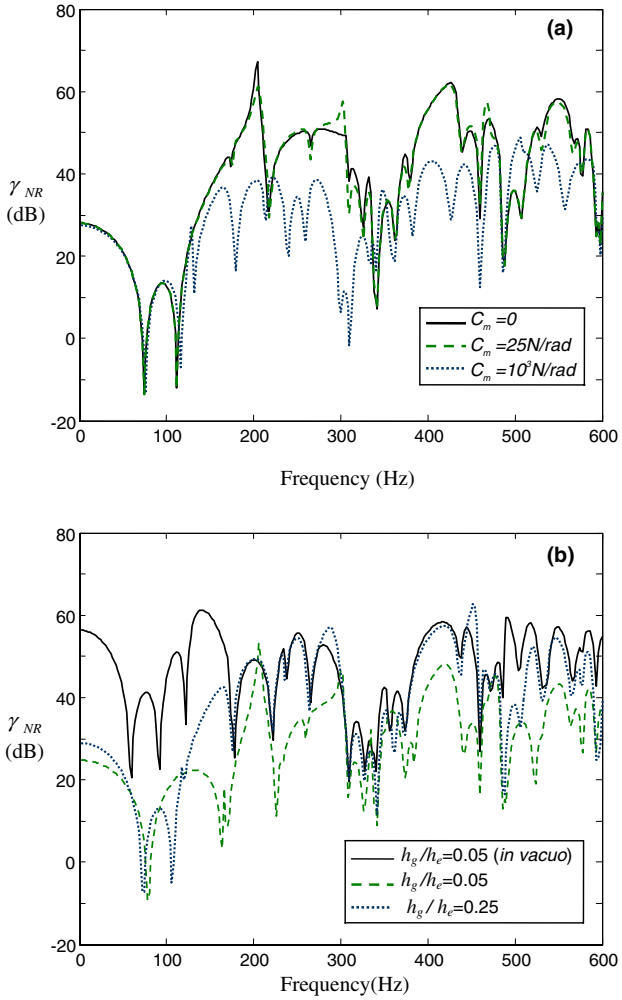

Fig. 4. Noise reduction index γ_{NR} ($h_g/h_e = 0.2$): (a) Rotational effect of the mechanical link; and (b) Effect of the depth of the gap.

band covering 0 to 200 Hz, and a higher band ranging from 400 to 600 Hz. Using three different gap depths $h_g/h_e = 0.1$, 0.2 and 0.5, Figs. 5(a) and 5(b) depict the variations of γ_{pl} with respect to λ_k for the higher frequency band and the lower one, respectively. For both frequency bands, γ_{pl} increases with the increase of λ_k, indicating an enhanced energy transmission through rotational moments when the link is getting stiffer. A comparison between Figs. 5(a) and 5(b) clearly shows that the increase rate of γ_{pl} at high frequencies is much higher than that at low frequencies. Taking the case of $h_g/h_e = 0.5$ (solid line, $K_g \approx 1.5 \times 10^4$ N/m) as an example, a change in λ_k between 10^{-5} and $10^{-0.5}$ leads to 26.1% increase in γ_{pl} in the higher frequency band (Fig. 5(a)), while only 8.9% in the lower one

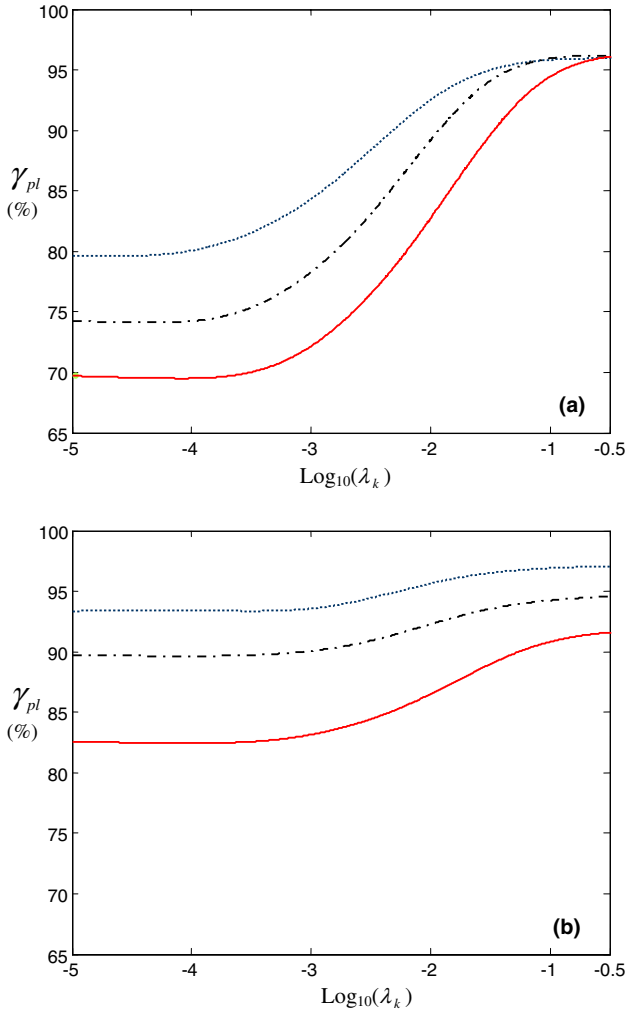

Fig. 5. Energy transmission between two walls for different h_g/h_e in the frequency region: (a) [400–600] Hz; and (b) [0–200] Hz. $h_g/h_e = 0.1$: ⋯; $h_g/h_e = 0.2$: -·-; $h_g/h_e = 0.5$: —.

(Fig. 5(b)). This observation implies a stronger rotational effect on energy transmission at high frequencies compared with lower ones. This is consistent with previous observations made on simple structures such as infinite beams or plates, whose rotational mobility increases with frequencies, whilst translational mobility usually keeps unchanged [13]. Both Figs. 5(a) and 5(b) also show that the variation of γ_{pl} is narrowed down when h_g/h_e is getting smaller. This is quite reasonable because, for a shallower gap, acoustic transmission becomes more dominant, such reducing the effect of the link.

3.4. Rotational effect vs. translational effect

Practical mechanical links provide energy transmission path through both translation and rotation simultaneously. An example is given in Fig. 6, when $h_g/h_e = 0.2$ ($K_g \approx 3.6 \times 10^4$ N/m), to show the effects of K_m and C_m on energy transmission. Different areas can be identified in which energy transmission process takes place through different paths. Given low K_m values, γ_{pl} moves from area I through II to III as C_m increases, basically following the same tendency as described in Section 3.1. Keeping C_m constant at small values and varying K_m result in a similar variation in γ_{pl} (areas I, IV and V), which is consistent with previous investigations [13]. Within these two strips, energy is transmitted either completely through the air gap (area I), or together with rotation (II and III) or translation (IV and V) of the link. The two strips denoted by III and V represent areas dominated by a strong rotational and translational link, respectively. Their intersection area VI corresponds to a very hard link in both rotation and translation. Note that the variation in γ_{pl} is rather smooth in these areas, the links can be regarded as rigid compared with the two panels. Area VII forms a complex region in which energy is transmitted through a combination of all possible paths (air gap, rotational and translational links).

In the presence of the translational effect, rotational effect on energy transmission in different frequency regions is revisited. Fig. 7 depicts the variations of γ_{pl} in the higher and lower frequency bands, when $K_m = 10^3$, 3×10^4 and 10^6 N/m. It can be seen that the general tendency of the curves is similar to Fig. 5. A pronounced rotational effect occurs in the higher frequency band, especially for the structure with a soft translational link, e.g., $K_m = 10^3$ N/m. With the increase of K_m, however, the variation of γ_{pl} significantly reduces, from 20% for $K_m = 10^3$ N/m (solid line) to 3% for $K_m = 10^6$ N/m(dotted line), indicating a much weaken rotational effect for stiff translational links.

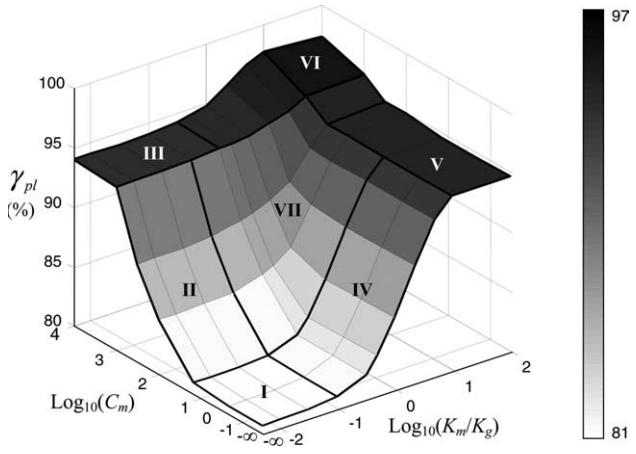

Fig. 6. Relationship between the rotational effect and the translational effect on energy transmission ($h_g/h_e = 0.2$).

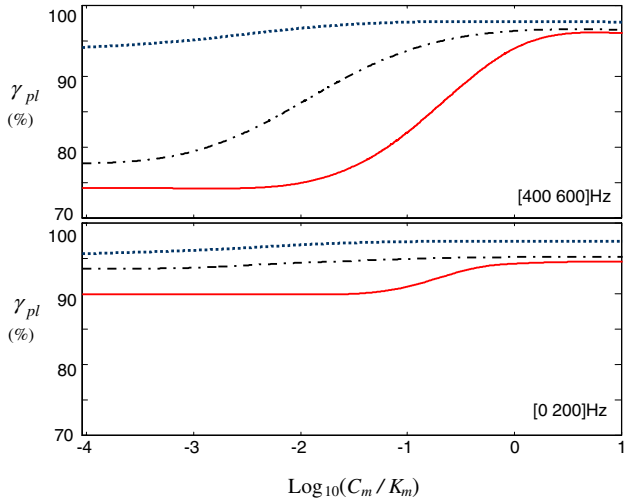

Fig. 7. Energy transmission between two walls ($h_g/h_e = 0.2$) for different K_m in the frequency region: (a) [400–600] Hz; and (b) [0–200] Hz. $K_m = 3 \times 10^4$ N/m: —; $K_m = 2 \times 10^5$ N/m: -·-; $K_m = 10^6$ N/m: ···.

4. Conclusions

Energy transmission through rotational effect of mechanical links in a double wall structure coupled with an acoustic enclosure was investigated in this paper. Based on a fully coupled vibroacoustic model, numerical simulations were performed with a view to establish a simple criterion for determining the most dominant path for energy transmission. The following conclusions can be drawn.

(1) The rotational effect of mechanical links on sound/vibration transmission of double-wall structures is obvious. It not only enhances the coupling between the two panels, but also intensifies the energy exchange between them, leading to an increased sound field in the enclosure, especially at higher frequencies.
(2) The rotational stiffness of the links and the aerostatic stiffness of the air gap are found to be the key parameters governing the energy transmission process. The ratio between the two stiffness terms, i.e., λ_k, can be used to roughly predict the dominant transmission path (acoustic or structural). Three zones are shown to exist in which different energy transmission mechanisms are involved. Energy is mainly transmitted from the acoustic path when $\lambda_k \subset (0\,0.001]$, from the structural path when $\lambda_k \subset [0.1\,\infty)$ or from both when $\lambda_k \subset [0.001\,0.1]$.
(3) The rotational effect exhibits much stronger influences on energy transmission at high frequencies due to the increasing mobility of the panels. This effect is further amplified when the double-wall structure has a soft translational link.

Acknowledgements

The authors would like to thank the Research Grants Council of Hong Kong Special Administrative Region (PolyU 5155/01E) for the financial support for this project. Support from The Hong Kong Polytechnic University to the second author is acknowledged (Project G-U136 and Special Fund for New Chair Professors).

Appendix

In the case of harmonic excitation, Eqs. (6), (7), (9) and (10) can be combined into matrix form as

$$\begin{bmatrix} H_{11} & H_{12} & H_{13} & 0 \\ H_{21} & H_{22} & H_{23} & H_{24} \\ H_{31} & H_{32} & H_{33} & 0 \\ 0 & H_{42} & 0 & H_{44} \end{bmatrix} \begin{Bmatrix} \mathbf{A} \\ \mathbf{B} \\ \mathbf{C} \\ \mathbf{D} \end{Bmatrix} = \begin{Bmatrix} \mathbf{F_a} \\ \mathbf{0} \\ \mathbf{0} \\ \mathbf{0} \end{Bmatrix}.$$

where

$$H_{11} = M_{\mathrm{a}} + K_{\mathrm{m}}\boldsymbol{\Phi}^{\mathrm{T}}(x_{\mathrm{m}}, y_{\mathrm{m}})\boldsymbol{\Phi}(x_{\mathrm{m}}, y_{\mathrm{m}}) + C_{\mathrm{m}}[\boldsymbol{\Psi}_x^{\mathrm{T}}(x_{\mathrm{m}}, y_{\mathrm{m}})\boldsymbol{\Psi}_x(x_{\mathrm{m}}, y_{\mathrm{m}}) - \boldsymbol{\Psi}_y^{\mathrm{T}}(x_{\mathrm{m}}, y_{\mathrm{m}})\boldsymbol{\Psi}_y(x_{\mathrm{m}}, y_{\mathrm{m}})],$$

$\boldsymbol{\Phi}(x_{\mathrm{m}}, y_{\mathrm{m}}) = [\varphi_{11}(x_{\mathrm{m}}, y_{\mathrm{m}}), \varphi_{12}(x_{\mathrm{m}}, y_{\mathrm{m}}), \ldots, \varphi_{\mathrm{MN}}(x_{\mathrm{m}}, y_{\mathrm{m}})]$, ($\varphi_{ij} = \varphi_{\mathrm{a},ij} = \varphi_{\mathrm{b},ij}$ for the two panels with same boundary condition)

$$\boldsymbol{\Psi}_x(x_{\mathrm{m}}, y_{\mathrm{m}}) = \left[\left.\frac{\partial\varphi_{11}(x,y)}{\partial x}\right|_{x=x_{\mathrm{m}},y=y_{\mathrm{m}}}, \ldots, \left.\frac{\partial\varphi_{\mathrm{MN}}(x,y)}{\partial x}\right|_{x=x_{\mathrm{m}},y=y_{\mathrm{m}}} \right],$$

$$\boldsymbol{\Psi}_y(x_{\mathrm{m}}, y_{\mathrm{m}}) = \left[\left.\frac{\partial\varphi_{11}(x,y)}{\partial y}\right|_{x=x_{\mathrm{m}},y=y_{\mathrm{m}}}, \ldots, \left.\frac{\partial\varphi_{\mathrm{MN}}(x,y)}{\partial y}\right|_{x=x_{\mathrm{m}},y=y_{\mathrm{m}}} \right],$$

$$H_{12} = -K_{\mathrm{m}}\boldsymbol{\Phi}^{\mathrm{T}}(x_{\mathrm{m}}, y_{\mathrm{m}})\boldsymbol{\Phi}(x_{\mathrm{m}}, y_{\mathrm{m}}) - C_{\mathrm{m}}\lfloor \boldsymbol{\Psi}_x^{\mathrm{T}}(x_{\mathrm{m}}, y_{\mathrm{m}})\boldsymbol{\Psi}_x(x_{\mathrm{m}}, y_{\mathrm{m}}) - \boldsymbol{\Psi}_y^{\mathrm{T}}(x_{\mathrm{m}}, y_{\mathrm{m}})\boldsymbol{\Psi}_y(x_{\mathrm{m}}, y_{\mathrm{m}})\rfloor,$$

$$H_{22} = M_{\mathrm{b}} + K_{\mathrm{m}}\boldsymbol{\Phi}^{\mathrm{T}}(x_{\mathrm{m}}, y_{\mathrm{m}})\boldsymbol{\Phi}(x_{\mathrm{m}}, y_{\mathrm{m}}) + C_{\mathrm{m}}\lfloor \boldsymbol{\Psi}_x^{\mathrm{T}}(x_{\mathrm{m}}, y_{\mathrm{m}})\boldsymbol{\Psi}_x(x_{\mathrm{m}}, y_{\mathrm{m}}) - \boldsymbol{\Psi}_y^{\mathrm{T}}(x_{\mathrm{m}}, y_{\mathrm{m}})\boldsymbol{\Psi}_y(x_{\mathrm{m}}, y_{\mathrm{m}})\rfloor.$$

The expressions of other terms, e.g., M_{a}, M_{b}, $H_{13}, \ldots$ and H_{44}, are the same as those presented in our previous work. The readers can refer to [13] for details.

References

[1] London A. Transmission of reverberant sound through double wall. J Acoust Soc Am 1950;22:270–9.
[2] Craik RJM, Smith RS. Sound transmission through double leaf lightweight partitions part I: airborne sound. Appl Acoust 2000;61(2):223–45.

[3] Grosveld FW, Shepherd KP. Active sound-attenuation across a double-wall structure. J Aircraft 1994;31:223–7.
[4] Sas P, Bao C, Augusztinovisz F, Desmet W. Active control of sound transmission through a double-panel partition. J Sound Vib 1995;180:609–25.
[5] Bao C, Pan J. Experimental study of different approaches for active control of sound transmission through double walls. J Acoust Soc Am 1997;102:1664–70.
[6] Wang CY, Vaicaitis R. Active control of vibrations and noise of double wall cylindrical shells. J Sound Vib 1998;216:865–88.
[7] Pan J, Bao C. Analytical study of different approaches for active control of sound transmission through double walls. J Acoust Soc Am 1998;103:1916–22.
[8] Gardonio P, Elliott SJ. Active control of structure-borne and airborne sound transmission through double panel. J Aircraft 1999;36:1023–32.
[9] Kaiser OE, Pietrzko SJ, Morari M. Feedback control of sound transmission through a double glazed window. J Sound Vib 2003;263:775–95.
[10] Carneal JP, Fuller CR. An analytical and experimental investigation of active structural acoustic control of noise transmission through double panel systems. J Sound Vib 2004;272:749–71.
[11] Lin GF, Garrelick JM. Sound transmission through periodically framed parallel plates. J Acoust Soc Am 1977;61:1014–8.
[12] Bao C, Pan J. Active acoustic control of noise transmission through double walls: effect of mechanical paths. J Sound Vib 1998;215:395–8.
[13] Cheng L, Li YY, Gao JX. Energy transmission in a mechanically-linked double-wall structure coupled to an acoustic enclosure. J Acoust Soc Am 2005;117(6):2742–51.
[14] Bouhioui H. Vibroacoustic study of a double glazing system. Université de Technologie de Compiègne, Compiègne, PhD Thesis, 1993 [in French].
[15] Skelton EA. Acoustic scattering by parallel plates with a single connector. Proc R Soc Lond A 1990;427:401–18.
[16] Brunskog J. The influence of finite cavities on the sound insulation of double-plate structures. J Acoust Soc Am 2005;117:3727–39.
[17] Petersson BAT, Gibbs BM. The influence of source location with respect to vibrational energy transmission. In: Proceeding of the 3rd international congress on intensity technique, Senlis, France. p. 449–56.
[18] Sanderson MA, Fredo CR, Ivarsson LI, Gillenang M. Transfer path analysis including internal force and moment strength estimations at vibration isolators, Newport Beach (CA), USA. In: Proceeding of inter-noise. p. 1407–10.
[19] Fulford RA, Petersson BAT. The role of moments on the vibration transmission in built-up structure. J Sound Vib 1999;227:479–510.
[20] Koh YK, White RG. Analysis and control of vibrational energy transmission to machinery supporting structures subjected to a multi-excitation system, Part I: driving point mobility matrix of beams and rectangular plates. J Sound Vib 1997;196(4):469–93.
[21] Gardonio P, Elliot SJ, Pinnington RJ. Active isolation of structural vibration on a multiple degree of freedom system, Part I: The dynamics of the system. J Sound Vib 1997;207:61–93.
[22] Goyder HGD, White RG. Vibrational power flow from machines into built-up structures, Part III: power flow through isolation systems. J Sound Vib 1980;68:97–117.
[23] Takahashi D. Sound radiation from periodically connected double-plate structures. J Sound Vib 1983;90:541–57.
[24] Dowell EH, Gorman GF, Smith DA. Acoustoelasticity: general theory, acoustic natural modes and forced response to sinusoidal excitation, including comparisons with experiment. J Sound Vib 1977;52:519–41.